Global Advanced Research Journal of Engineering, Technology and Innovation (ISSN: 2315-5124) Vol. 1(9) pp. 236-251, December, 2012
Available online http://garj.org/garjeti/index.htm

Full Length Research Paper

Controlling the Vehicle Disc Brake Squeal Using A 10 DOF Model

Ibrahim Ahmed[1] and Yasser Fatouh[1]

[1]Department of Automotive Technology, Faculty of Industrial Education, Helwan University, Cairo, EGYPT

Accepted 20 December 2012

The disc brake squeal generated during the duty of the brake is considered as a highly main source of discomfort for passengers. It is also considered to be a high frequency noise when it is bigger than 1 kHz audible vibration of braking components which is a significant problem that has not been solved satisfactorily until recently. Squeal noise is strongly correlated to the squeal index and degree of instability of the brake system assembly. Decreasing or controlling this squeal noise to some extent during braking is very important matter for the comfort of passengers. So, a mathematical prediction model of 10-degree-of-freedom has been developed to study the effect of different brake components parameters on the degree of instability and squeal index of the brake system. The model has considered such factors as the distance between clamping bolts of the caliper and width of the friction material, which were not fully covered previously besides some other factors. In this paper, the system is considered to be completely state controllable and hence it will be "observable", then poles of the closed-loop system will be placed at a desired location by means of state feedback through the state feedback gain matrix. This term of observability is found to be important because, in practice, the difficulty encountered with state feedback control is that some of the state variables are not accessible for direct measurement, with the result that it becomes necessary to estimate the immeasurable state variable in order to construct the control signals. Complex eigenvalue analysis and state-space representation of the model have been solved using a MATLAB program. It is evident from the analysis that Young's moduli of the rotor and friction material have a great effect on the occurrence of squeal. The harder the friction material the bias of the brake to squeal. It is shown also that the squeal noise of the brake decreases with increasing semi-distance between the clamping bolts of the caliper to be at optimum value between 50-70 mm. The results have show that the predicted squeal tendency at varying all the studies parameters with feedback control signal is as less as possible to be 43 % compared to other single parameters without feedback signal.

Keywords: Ventilated disc brake, brake, squeal, SI, degree of instability, eigen frequency, controllable and observable.

INTRODUCTION

The theory of the brake squeal noise has attracted the attention many years ago because of the complex dynamic problem during the duty of the brake. Since vehicle comfort has become an important factor to indicate the quality of a passenger car, so, eliminating or reducing the noise and vibration of a vehicle structure and system seems to provide a leading edge in the

*Corresponding author Email: ilmahmed1968@yahoo.co.uk

market to vehicle manufacturers (Saw Chun *et al.,* 2009 and Ahmed, 2012). Many manufacturers of brake pad materials spend up to 50% of their engineering budgets on noise, vibration and harshness (NVH) issues (Kinkaid *et al.,* 2003). Generally in disc brakes, squeal can occur when the brake pads contact the rotor while the vehicle is moving at low speeds, setting up a vibration that manifests itself as an annoying high-pitched squeal. market to vehicle manufacturers (Saw Chun *et al.,* 2009 and Ahmed, 2012). Many manufacturers of brake pad materials spend up to 50% of their engineering budgets on noise, vibration and harshness (NVH) issues (Kinkaid *et al.,* 2003). Generally in disc brakes, squeal can occur when the brake pads contact the rotor while the vehicle is moving at low speeds, setting up a vibration that manifests itself as an annoying high-pitched squeal.

Many researchers in their studies on the dynamics of brake system tried to reduce squeal by changing the factors associated with the brake squeal or modifying the brake rotor experimentally and theoretically. (Gouyan *et al.,* 1990) studied the low frequency groan of the brake that occurs due to the increase in the disc temperature. It was observed that the groan noise is an oscillatory phenomenon, which occurs from the effect of vibrations on the friction force between a disc and a pad during coupling of two rotational vibrations of a disc caliper. (Nishiwaki *et al.,* 1989) studied the squeal experimentally and theoretically by modifying the disc (rotor) to eliminate brake squeal that occurred by self-excited vibration. The vibration modes during brake squeal generation at 6.32 kHz and 8.25 kHz were visualized by Holographic Interferometry. However, the conventional disc (rotor) vibrates at the maximum amplitude in the area excited artificially. (Liles, 1989) found that shorter pads, damping, softer disc and stiffer back plate could reduce squeal whilst in contrast, higher friction coefficient and wear of the friction material were prone to squeal. (Lee *et al.,* 1998) reported that reducing back plate thickness led to less uniform of contact pressure distributions and consequently increasing the squeal propensity. (Hu *et al.,* 1999) found the optimal design of experiments analysis was the one that used the original finger length, the vertical slot, the chamfer pad, the 28mm thickness of disc, and the 10mm thickness of friction material.

(Shin et al., 2002) have shown that the damping of the pad and the disc were important in reducing instability. Their analysis also has shown and confirmed that increasing damping of either the disc or the pad alone could potentially destabilize the system. (Liu et al., 2007) found that the squeal can be reduced by decreasing the friction coefficient, increasing the stiffness of the disc, using damping material on the back of the pads and modifying the shape of the brake pads. (Dai *et al.,* 2008) have shown that the design of the pads with a radial chamfer possesses the least number of unstable modes, which implies lesser tendency towards squeal. (Ahmed et al., 2008 and 2009) have shown the effect of disc and pad surface modification by adding a slot in the middle of the pad had a great effect on the reducing of the brake squeal through the escape of the wear particle via this slot.

The squeal of the disc brake has been studied experimentally by installing accelerometers on the back-plate of the pad. It was observed that the higher the coefficient of friction, the more the rotor squeals (Yasuaki *et al*., 1993). A brake dynamometer was used also to study the brake squeal by knowing the intensity and duration of the squeal and also the frequency range of the squeal. In this study, the pressure, temperature, and speed ranges were fully controlled during the occurrence of the squeal (Bracken *et al.,* 1982). (Earles *et al.,* 1988) dealt with the squeal as not a serious problem considering that the squealing brake provides more effective braking than a non-squealing brake. It was concluded that increasing disc damping and allowing a decrease in rotor stiffness would appear to produce the most benefit of decreasing the squeal noise generation. (Millner, 1978) dealt with the squeal theoretically by studying the first eight disc mode instabilities at μ (coefficient of friction) less than 0.5 by building a multi degree of freedom mathematical model. The lower value of linear stiffness of the caliper of 318 MNm^{-1} to give instability was obtained at the third mode. In a separate piece of work a new system was developed to stop the squeals by (Nishizawa *et al*., 1997) by evaluating the electronic control cancelling for the noise (ECCN) with the test vehicle. The ECCN was installed in both front calipers to stop the frequency squeals (2-4 KHz) by decreasing the rotor vibration electronically on both the noise dynamometer and the test vehicle. (Thomas *et al.,* 1998) studied the effect of the support stiffness and damping conditions on the measured modal parameters as frequencies and damping ratios. It was realized that the increase of the measured frequency of the supported system was related to the square of the frequency ratio of the rigid body mode and the elastic mode.

It is clear then from those issues that; there were no recommendations for reducing the squeal of the disc brake from the point of view of the control system dynamic. In the following model of the disc brake there is incorporation with the relevant parts of these theories according to the theory of system dynamic. This paper is focusing on decreasing the squeal of the ventilated fixed caliper disc brake which has not been mathematically covered previously using a ten-degree-of-freedom model. The system is considered to be completely state controllable and hence it will be “observable”, then poles of the closed-loop system will be placed at a desired location by means of state feedback through the state feedback gain matrix. This term of observability is found to be important because, in practice, the difficulty encountered with state feedback control is that some of the state variables are not accessible for direct measurement, with the result that it becomes necessary

to estimate the immeasurable state variable in order to construct the control signals. The designed model has taken such factors as the distance between clamping bolts of the caliper, weight of the caliper and thicknesses of the rotor rings that were not fully covered in most literatures. In addition to some other factors such as width and Young's Modulus of the friction material and rotor that can affect the brake stability and consequently brake squeal noise.

Mathematical Model of the Ventilated Disc Brake Squeal Noise

It is well-known that in the fixed caliper disc brake type, the caliper piston presses the right (inner) and left (outer) pads towards the ventilated rotor at the same time as shown in Figure 1. So, a lag could be occurring between the two pads at pressing on the rotor and it is assumed that the forces occur at the same time and there is a fully contact between the pads and the rotor. A theoretical 10-degree-of-freedom mathematical model has been developed in this study depending on the theoretical model of (North, 1972 and Millner, 1978) who are the pioneers of dealing with the brake squeal mathematically and also the model of (Ahmed, 2012). This mathematical model stresses mainly on changing some brake parameters properties in order to find a formula valid for minimizing the brake squeal as less as possible as clear later.

The stability of the system of equations, according to the geometric stability hypothesis, reflects the likelihood

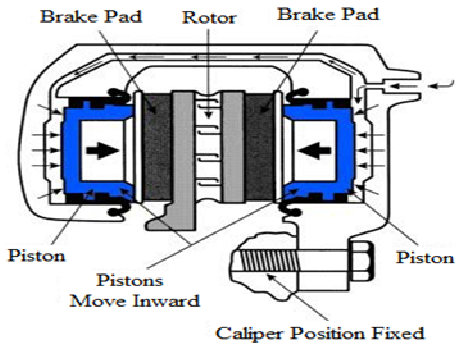

Figure 1. Ventilated disc brake rotor (Crolla, 2009).

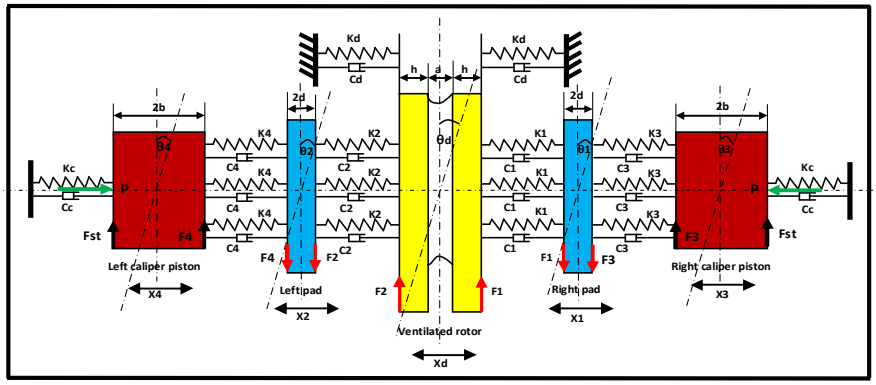

Figure 2. Theoretical ten-degree-of-freedom mathematical model for ventilated disc brake, (North, 1972, Millner, 1978, Wagner *et al.,* 2004 and Neubauer *et al.,* 2008)

of squeal for the brake system modeled (Mario Triches *et al.,* 2008). Several techniques for evaluating the stability of a system are available.

Approaches considered were (a) A transient solution of the dynamic equations of motion, (b) Evaluation of the Routh criterion, and (c) An eigenvalue analysis of the system. A divergent transient solution indicates that instabilities are present in the system. Likewise, the Routh criterion demonstrates whether or not a system is stable. Such solutions, however, provide no insight into how the structure could be altered to remove the instability. On the other hand, the complex roots obtained from an eigenvalue analysis can reveal which system vibration modes are unstable. Knowledge of the

unstable system modes facilitates several control methods: modal frequencies could be moved by changing components or adding damping, so that the mode in question becomes stable. Based on the usefulness of the information, complex eigenvalues using MATLAB program are used as a measure of the system stability. It is known that the equation of motion of a linear system is:

$$[M]\{\ddot{u}\}+[C]\{\dot{u}\}+[K]\{u\}=\{F\} \quad (1)$$

Where M, C and K are mass, damping and stiffness matrices, respectively, and u is the generalized displacement vector. For friction induced vibration, it is assumed that the forcing function F is mainly contributed by the variable friction force at the pad–rotor interface.
The friction interface is modeled as an array of friction springs and dampers as shown in Figure 2. With this simplified interface model, the force vector becomes linear. Based on Newton's second law, the equations of motion of the mathematical model of ventilated disc brake shown in figure 2 for a constant pressure P can be written after considering some assumptions including:

- The system is state controllable.
- The ventilated rotor has two degrees of freedom, one in the x-axis direction and the other around the y-axis direction.
- Each pad has two degrees of freedom, one in the x-axis direction and the other around the y-axis direction.
- Each piston has two degrees of freedom, one in the x-axis direction and the other around the y-axis direction.
- The contact forces *F1, F2, F3 and F4* are parallel to the face of the rotor, pads and pistons as shown in figure 2 and will be activated during the contact between the pads and the rotor.
- The rotor and the pads vibrate in the same mode.

The equations of motion of the ventilated disc due to translational and rotational displacements x_d and θ_d are summarized as follow:

$$\begin{aligned} &M_d.\ddot{x}_d+(C_1+C_2+C_D).\dot{x}_d-C_1.\dot{x}_1-C_2.\dot{x}_2 \\ &\quad+(K_1+K_2+K_D).x_d-K_1.x_1-K_2.x_2 \\ &\quad+(F1+F2).\theta_d=0 \end{aligned} \quad (2)$$

$$\begin{aligned} &I_d.\ddot{\theta}_d+(C_5+C_6+C_{DR}).\dot{\theta}_d-C_5.\dot{\theta}_1-C_6.\dot{\theta}_2 \\ &\quad+(K_5+K_6+K_{DR}).\theta_d-K_5.\theta_1-K_6.\theta_2 \\ &\quad+(F1+F2).(h+\frac{a}{2})=0 \end{aligned} \quad (3)$$

The equations of motion of the right pad due to translational and rotational displacements x_1 and θ_1 are summarized as follow:

$$\begin{aligned} &M_1.\ddot{x}_1-C_1.\dot{x}_d+(C_1+C_3).\dot{x}_1-C_3.\dot{x}_3-K_1.x_d \\ &\quad+(K_1+K_3).x_1-K_3.x_3+(F1-F3).\theta_1=0 \end{aligned} \quad (4)$$

$$\begin{aligned} &I_1.\ddot{\theta}_1-C_5.\dot{\theta}_d+2C_5.\dot{\theta}_1-C_5.\dot{\theta}_3-K_5.\theta_d+2K_5.\theta_1 \\ &\quad-K_5.\theta_3-(F1+F3).d=0 \end{aligned} \quad (5)$$

The equations of motion of the left pad due to translational and rotational displacements x_2 and θ_2 are summarized as follow:

$$\begin{aligned} &M_2.\ddot{x}_2-C_2.\dot{x}_d+(C_2+C_4).\dot{x}_2-C_4.\dot{x}_4 \\ &\quad-K_2.x_d+(K_2+K_4).x_2-K_4.x_4 \\ &\quad+(F2-F4).\theta_2=0 \end{aligned} \quad (6)$$

$$\begin{aligned} &I_2.\ddot{\theta}_2-C_6.\dot{\theta}_d+2C_6.\dot{\theta}_2-C_6.\dot{\theta}_4-K_6.\theta_d \\ &\quad+2K_6.\theta_2-K_6.\theta_4-(F2+F4).d=0 \end{aligned} \quad (7)$$

The equations of motion of the right piston caliper due to translational and rotational displacements x_3 and θ_3 are summarized as follow:

$$\begin{aligned} &M_C.\ddot{x}_3+(C_3+Cc).\dot{x}_3-C_3.\dot{x}_1+(K_3+Kc).x_3 \\ &\quad-K_3.x_1+(F3+Fst).\theta_3=0 \end{aligned} \quad (8)$$

$$\begin{aligned} &I_3.\ddot{\theta}_3-C_7.\dot{\theta}_1+(C_7+C_{RC}).\dot{\theta}_3-K_7.\theta_1 \\ &\quad+(K_7+K_{RC}).\theta_3+(F3+Fst).b=0 \end{aligned} \quad (9)$$

The equations of motion of the left piston caliper due to translational and rotational displacements x_4 and θ_4 are summarized as follow:

$$\begin{aligned} &M_C.\ddot{x}_4+(C_4+Cc).\dot{x}_4-C_4.\dot{x}_2+(K_4+Kc).x_4 \\ &\quad-K_4.x_2+(F4+Fst).\theta_4=0 \end{aligned} \quad (10)$$

$$\begin{aligned} &I_4.\ddot{\theta}_4-C_8.\dot{\theta}_2+(C_8+C_{RC}).\dot{\theta}_4-K_8.\theta_2 \\ &\quad+(K_8+K_{RC}).\theta_4+(F4+Fst).b=0 \end{aligned} \quad (11)$$

Where

$$F1=\mu.R_1=\mu.[F_{st}+C_1.(\dot{x}_d-\dot{x}_1)+K_1.(x_d-x_1)] \quad (12)$$

$$F2=\mu.R_2=\mu.[F_{st}+C_2.(\dot{x}_d-\dot{x}_2)+K_2.(x_d-x_2)] \quad (13)$$

$$F3=\mu.R_3=\mu_b.[F_{st}+C_3.(\dot{x}_3-\dot{x}_1)+K_3.(x_3-x_1)] \quad (14)$$

$$F4=\mu.R_4=\mu_b.[F_{st}+C_4.(\dot{x}_4-\dot{x}_2)+K_4.(x_4-x_2)] \quad (15)$$

The equations from (2) to (11) can be rewritten in the

form of:

$$[\ddot{x}]+[c]/[m].[\dot{x}]+[\mathrm{k}]/[\mathrm{m}].[x]=0 \quad (16)$$

$$[\ddot{x}]+[2.\zeta.\omega_n][\dot{x}]+[\omega_n^2][x]=0 \quad (17)$$

Where

ω_n is the natural frequency of the system.

ζ is the damping ratio or viscous damping factor and equal to ζ=c/2.m. ω_n

The solutions will be assumed to be in the form as follows:

$X_d = A_d . e^{\lambda t}$ and $\theta_d = B . e^{\lambda t}$
due to disc displacement and rotation.

$X_1 = C . e^{\lambda t}$ and $\theta_1 = D . e^{\lambda t}$
due to right pad displacement and rotation.

$X_2 = E . e^{\lambda t}$ and $\theta_2 = F . e^{\lambda t}$
due to left pad displacement and rotation.

$X_3 = G . e^{\lambda t}$ and $\theta_3 = H . e^{\lambda t}$
due to right caliper piston displace. and rotation

$X_4 = I . e^{\lambda t}$ and $\theta_4 = J . e^{\lambda t}$
due to left caliper piston displace.and rotation.

And by substitution in the main equation, the characteristic equation can be expressed in the following form:

$$\lambda^2 + 2.\zeta.\omega_n.\lambda + \omega_n^2 = 0 \quad (18)$$

And the roots of this equation will appear as a complex conjugate pairs as follows:

$$\lambda 1 = \omega_n.(-\zeta + \sqrt{(\zeta^2 - 1).})$$

and $$\lambda 2 = \omega_n.(-\zeta - \sqrt{(\zeta^2 - 1).})$$

The displacement can be also rewritten as a damped sinusoidal wave in the form of:

$$\{u_i\} = \{\phi_i\} e^{\sigma_i t} \cos \omega_i t \quad (19)$$

Thus, σ_i and ω_i are the damping coefficient and damped natural frequency describing damped sinusoidal motion.

By examining the real part of the system eigenvalues the modes that are unstable and likely to produce squeal are revealed. Generally, disc brake squeal is caused by unstable vibrations of the brake system. A Matlab program is used to determine if the brake system will squeal or not by checking the stability of the ventilated disc brake assembly. This program is able to carry out the eigenvalue analysis that can indicate the instability level and the natural frequency. The corresponding eigenvalue problem will be in the form of $d\ (\lceil A \rceil - \lambda \lceil I \rceil) = 0$. Each eigenvalue λ is a complex number that contains two parts as mentioned earlier. The first part is real and the second part is imaginary. When the real part is negative, this indicates that the mode is damped and stable and when the real part is positive, it means that the mode is not stable and the damping is negative. Rearranging these equations (2-11) to be as in the form of equation (1); the mass matrix [M] will be in the form of:

$$[M] = \begin{bmatrix} M_d & 0 & 0 & 0 & 0 & 0 & 0 & 0 & 0 & 0 \\ 0 & I_d & 0 & 0 & 0 & 0 & 0 & 0 & 0 & 0 \\ 0 & 0 & M_1 & 0 & 0 & 0 & 0 & 0 & 0 & 0 \\ 0 & 0 & 0 & I_1 & 0 & 0 & 0 & 0 & 0 & 0 \\ 0 & 0 & 0 & 0 & M_2 & 0 & 0 & 0 & 0 & 0 \\ 0 & 0 & 0 & 0 & 0 & I_2 & 0 & 0 & 0 & 0 \\ 0 & 0 & 0 & 0 & 0 & 0 & M_3 & 0 & 0 & 0 \\ 0 & 0 & 0 & 0 & 0 & 0 & 0 & I_3 & 0 & 0 \\ 0 & 0 & 0 & 0 & 0 & 0 & 0 & 0 & M_4 & 0 \\ 0 & 0 & 0 & 0 & 0 & 0 & 0 & 0 & 0 & I_4 \end{bmatrix}.$$

And the damping matrix [C] will be in the form of:

$$[C]=\begin{bmatrix}
(C_1+C_2+C_D) & 0 & -C_1 & 0 & -C_2 & 0 & 0 & 0 & 0 & 0 \\
0 & (C_5+C_6+C_{DR}) & 0 & -C_5 & 0 & -C_6 & 0 & 0 & 0 & 0 \\
-C1 & 0 & (C_1+C_3) & 0 & 0 & 0 & -C_3 & 0 & 0 & 0 \\
0 & -C_1 & 0 & 2C_5 & 0 & 0 & 0 & C_5 & 0 & 0 \\
-C2 & 0 & 0 & 0 & (C_2+C_4) & 0 & 0 & 0 & -C_4 & 0 \\
0 & -C_6 & 0 & 0 & 0 & 2C_6 & 0 & 0 & 0 & -C_6 \\
0 & 0 & -C_3 & 0 & 0 & 0 & (C_3+Cc) & 0 & 0 & 0 \\
0 & 0 & 0 & -C_7 & 0 & 0 & 0 & (C_7+C_{RC}) & 0 & 0 \\
0 & 0 & 0 & 0 & -C_4 & 0 & 0 & 0 & (C_4+Cc) & 0 \\
0 & 0 & 0 & 0 & 0 & -C_8 & 0 & 0 & 0 & (C_8+C_{RC})
\end{bmatrix}.$$

And the stiffness matrix [K] will be in the form of:

$$[K]=\begin{bmatrix}
(K_1+K_2+K_D) & (F1+F2) & -K_1 & 0 & -K_2 & 0 & 0 & 0 & 0 & 0 \\
0 & (K_5+K_6+K_{DR}) & 0 & -K_5 & 0 & -K_6 & 0 & 0 & 0 & 0 \\
-K_1 & 0 & (K_1+K_3) & (F1-F3) & 0 & 0 & -K_3 & 0 & 0 & 0 \\
0 & -K_5 & 0 & 2K_5 & 0 & 0 & 0 & K_5 & 0 & 0 \\
-K_2 & 0 & 0 & 0 & (K_2+K_4) & (F2+F4) & 0 & 0 & -K_4 & 0 \\
0 & -K_6 & 0 & 0 & 0 & 2K_6 & 0 & 0 & 0 & -K_6 \\
0 & 0 & -K_3 & 0 & 0 & 0 & (K_3+Kc) & (F3+Fst) & 0 & 0 \\
0 & 0 & 0 & -K_7 & 0 & 0 & 0 & (K_7+K_{RC}) & 0 & 0 \\
0 & 0 & 0 & 0 & -K_4 & 0 & 0 & 0 & (K_4+Kc) & (F4+Fst) \\
0 & 0 & 0 & 0 & 0 & -K_8 & 0 & 0 & 0 & (K_8+K_{RC})
\end{bmatrix}.$$

From the eigenvalues analysis, the instability levels and the eigenfrequencies are calculated. The instability level (degree of instability) is defined as the real part of the eigenvalue $\alpha = Re[\lambda]$ and the eigenfrequency is defined as the imaginary part of the eigenvalue $\omega = Im[\lambda]$ Hz. Some authors took the instability level as a squeal propensity and others don't. In this work the squeal propensity (σ) that is the squeal index will be taken as

$\sigma = \left(\alpha^2+\omega^2\right)^{1/2}.\sin\left(\delta/2\right)$ as Millner's, (1978) assumption and the results agree with it. The eigen frequencies will be taken as $\omega/2\pi$ Hz. Where δ is the phase angle.

$$\delta = \tan^{-1}\left(\frac{\text{Imaginary part}}{\text{Real part}}\right) \qquad \textbf{(22)}$$

SYSTEM CONTROL DESIGN

The dynamic behaviour of the closed-loop system is predicted by means of the open-loop frequency response. Generally, the dynamic behaviour of any complex system can be improved through inserting of a simple lead or a compensator. The techniques of conventional control theory are conceptually simple and require only reasonable amount of computation; the input, the output, and error signals are considered important in the control theory. The system designed by conventional control theory depends on trial and error procedures that will not yield optimal control systems. On the other hand, the system designed by the modern control theory particularly by state-space enables designing such systems having desired closed-loop poles or optimal control systems with respect to given performance index.

However, the design by modern control theory through state-space methods requires accurate mathematical description of the system dynamics. The performance index is a function whose value indicates how well the actual performance of the system matches the desired performance. In most cases, the control vector which is in the form of u=-Kx (where u is unconstrained) is chosen in such a way that the performance index is minimized or

Table 1. Ventilated disc brake rotor and pad specifications.

Properties and dimensions	Ventilated disc		Properties and dimensions	Pad (friction material	
Young's modulus, *Ed*	195	GN/m^2	Young's modulus, *Ep*	900	MN/m^2
Density, ρ	7600	kg/m^3	Density, ρ_p	2600	kg/m^3
Poisson's ratio, ν	0.27		Poisson's ratio, ν	0.23	
Coefficient of friction, μ	0.42		Coefficient of friction, μ	0.42	
Rings inner radius, r_i	70	mm	Backplate length,	128	mm
Rings outer radius, r_o	128	mm	Backplate thickness,	5	mm
Lower ring thickness, h	7	mm	Backplate width,	48	mm
Upper ring thickness, h	8	mm	Abutment width,	10	mm
Hub inner radius, h_i	32	mm	Abutment length,	8	mm
Hub outer radius, h_o	70	mm	Friction material length, 1	110	mm
Hub thickness, h_t	6	mm	Friction material thickness, 2d	10	mm
Hub length, h_l	22.4	mm	Friction material width, w	44	mm
Fins thickness, a	8	mm			

maximized optimizes the system behaviour. In this case the performance index will be written as follows

Performance index = $\sum_{i=1}^{n} (\mu_i - s_i)^2$, (Ogata, 1998).

Where the μ_i's are the desired eigenvalues of the error dynamics of the system and the S_i's are the actual eigenvalues of the error dynamics of the designed

For the input parameters (states);

$x_d = X_1$, $\dot{x}_d = X_2 = \dot{X}_1$,

$\theta_d = X_3$ $\dot{\theta}_d = X_4 = \dot{X}_3$

$x_1 = X_5$, $\dot{x}_1 = X_6 = \dot{X}_5$,

$\theta_1 = X_7$, $\dot{\theta}_1 = X_8 = \dot{X}_7$

$x_2 = X_9$, $\dot{x}_2 = X_{10} = \dot{X}_9$,

$\theta_2 = X_{11}$, $\dot{\theta}_2 = X_{12} = \dot{X}_{11}$

$x_3 = X_{13}$, $\dot{x}_3 = X_{14} = \dot{X}_{13}$,

$\theta_3 = X_{15}$, $\dot{\theta}_3 = X_{16} = \dot{X}_{15}$

$x_4 = X_{17}$, $\dot{x}_4 = X_{18} = \dot{X}_{17}$,

$\theta_4 = X_{19}$, $\dot{\theta}_4 = X_{20} = \dot{X}_{19}$

And assuming also for the output parameters;

$Y_1 = x_d = X_1$ $Y_2 = \theta_d = X_3$

$Y_3 = x_1 = X_5$ $Y_4 = \theta_1 = X_7$

$Y_5 = x_2 = X_9$ $Y_6 = \theta_2 = X_{11}$

$Y_7 = x_3 = X_{13}$ $Y_8 = \theta_3 = X_{15}$

$Y_9 = x_4 = X_{17}$ $Y_{10} = \theta_4 = X_{19}$

And by substitution in the equations of motion (2-11), the equations can be represented into the form as follows in the next equations (23-32);

$$\dot{X}_2 = -\left(\frac{K_1 + K_2 + K_D}{M_d}\right).X_1 - \left(\frac{C_1 + C_2 + C_D}{M_d}\right).X_2 - \left(\frac{F1 + F2}{M_d}\right).X_3 + \left(\frac{K_1}{M_d}\right).X_5 + \left(\frac{C_1}{M_d}\right).X_6 - \left(\frac{K_2}{M_d}\right).X_9 + \left(\frac{C_2}{M_d}\right).X_{10}$$

$$\dot{X}_4 = -\left(\frac{K_5 + K_6 + K_{DR}}{I_d}\right).X_3 - \left(\frac{C_5 + C_6 + C_{DR}}{I_d}\right).X_4 + \left(\frac{K_5}{I_d}\right).X_7 + \left(\frac{C_5}{I_d}\right).X_8 + \left(\frac{K_6}{I_d}\right).X_{11} + \left(\frac{C_6}{I_d}\right).X_{12} - \left(\frac{F1 + F2}{I_d}\right).(h + \frac{a}{2})$$

$$\dot{X}_6 = \left(\frac{K_1}{M_1}\right).X_1 + \left(\frac{C_1}{M_1}\right).X_2 - \left(\frac{K_1 + K_3}{M_1}\right).X_5 - \left(\frac{C_1 + C_3}{M_1}\right).X_6 - \left(\frac{F1 - F3}{M_1}\right).X_7 + \left(\frac{K_3}{M_1}\right).X_{13} + \left(\frac{C_3}{M_1}\right).X_{14}$$

$$\dot{X}_8 = \left(\frac{K_5}{I_1}\right).X_3 + \left(\frac{C_5}{I_1}\right).X_4 - \left(\frac{2.K_5}{I_1}\right).X_7 - \left(\frac{2.C_5}{I_1}\right).X_8 + \left(\frac{K_5}{I_1}\right).X_{15} + \left(\frac{C_5}{I_1}\right).X_{16} + \left(\frac{F1+F3}{I_1}\right).d$$

$$\dot{X}_{10} = \left(\frac{K_2}{M_2}\right).X_1 + \left(\frac{C_2}{M_2}\right).X_2 - \left(\frac{K_1+K_4}{M_2}\right).X_9 - \left(\frac{C_1+C_4}{M_2}\right).X_{10} - \left(\frac{F2-F4}{M_2}\right).X_{11} + \left(\frac{K_4}{M_2}\right).X_{17} + \left(\frac{C_4}{M_2}\right).X_{18}$$

$$\dot{X}_{12} = \left(\frac{K_6}{I_2}\right).X_3 + \left(\frac{C_6}{I_2}\right).X_4 - \left(\frac{2.K_6}{I_2}\right).X_{11} - \left(\frac{2.C_6}{I_2}\right).X_{12} + \left(\frac{K_6}{I_2}\right).X_{19} + \left(\frac{C_6}{I_2}\right).X_{20} + \left(\frac{F2+F4}{I_2}\right).d$$

$$\dot{X}_{14} = \left(\frac{K_3}{M_C}\right).X_5 + \left(\frac{C_3}{M_C}\right).X_6 - \left(\frac{K_3+Kc}{M_C}\right).X_{13} - \left(\frac{C_3+Cc}{M_C}\right).X_{14} - \left(\frac{F3+Fst}{M_C}\right).X_{15}$$

$$\dot{X}_{16} = \left(\frac{K_7}{I_3}\right).X_7 + \left(\frac{C_7}{I_3}\right).X_8 - \left(\frac{K_7+K_{RC}}{I_3}\right).X_{15} - \left(\frac{C_7+C_{RC}}{I_3}\right).X_{16} - \left(\frac{F3+Fst}{I_3}\right).b$$

$$\dot{X}_{18} = \left(\frac{K_4}{M_C}\right).X_9 + \left(\frac{C_4}{M_C}\right).X_{10} - \left(\frac{K_4+Kc}{M_C}\right).X_{17} - \left(\frac{C_4+Cc}{M_C}\right).X_{18} - \left(\frac{F4+Fst}{M_C}\right).X_{19}$$

$$\dot{X}_{20} = \left(\frac{K_8}{I_4}\right).X_{11} + \left(\frac{C_8}{I_4}\right).X_{12} - \left(\frac{K_8+K_{RC}}{I_4}\right).X_{19} - \left(\frac{C_8+C_{RC}}{I_4}\right).X_{20} - \left(\frac{F4+Fst}{I_4}\right).b$$

By substitution of the matrices by the data given in Table 1 and rearranging the equations of motion (2-11), it will lead to the state space method as shown in the next form of:

$$\dot{X} = AX + Bu. \quad (33)$$

$$Y = CX + Du. \quad (34)$$

Where

A is the System 20×20 matrix.
B is the Input 20×1 matrix.
C is the Output 10×20.
X is the System State 20-vector.
u is the Input vector.

And by examining the real part of the system eigenvalues using MATLAB program, the modes that are unstable and likely to produce squeal are revealed.

DESIGN THROUGH POLE PLACEMENT

The state space is concerned with three types of variables that are involved generally in the dynamic systems, which are input variables, output variables, and state variables. Generally, if the dynamic system is linear and time invariant the state-space equations will be in the form as mentioned in equations 33, and 34. The state feedback control scheme, which is the relationship between the output and reference input by comparing them and using the difference as a means of control is called feedback control system, is given by

$$u = - K x \quad (35)$$

Where u is the control signal (control vector).

The system is assumed to be completely state controllable. This means that, the control signal is determined as an instantaneous state and the 1×n matrix K is called the state feedback gain matrix. In the closed-loop control system as in figure (3), the actuating error signal, which is the difference between the input signal, and the feedback signal is fed to the controller to reduce the error and bring the output of the system to a desired value.

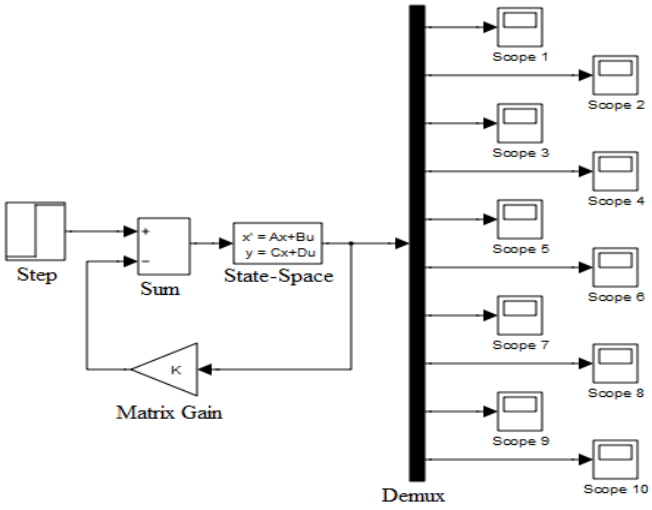

Figure 3. State-space of the ventilated disc brake with feedback control.

And by substitution by equation (35) in equation (33) gives:

$\dot{x}$ (t) = (A-BK).x (t) (36)

And the solution of this equation will be in the form of

x(t) = $e^{(A-BK)}$. x(0) (37)

Where **x(0)** is the initial state caused by external disturbances. The stability and transient response characteristics are determined by the eigenvalues of matrix A-BK. The eigenvalues of the matrix **(A-BK)** are called the regulator poles. If these regulator poles are located in the left-half of s plane, then **x(t)** approaches zero while t approaches infinity. Placing the closed-loop poles at the desired location is called a pole placement method. It is possible to transform the state equation given by equation (33) into the controllable canonical form. The transformation matrix T given in the form of

T = M.W (38)

Where M is the controllability matrix and given by

M = [B AB A^2 B A^3 B A^4 B …….. A^{19} B] (39)

And W is given in the form of;

$$W = \begin{bmatrix} a_{19} & a_{18} & a_{17} & \ldots\ldots\ldots\ldots a_1 & 1 \\ a_{18} & a_{17} & a_{16} & \ldots\ldots\ldots\ldots 1 & 0 \\ a_{17} & a_{16} & a_{15} & \ldots\ldots\ldots\ldots 0 & 0 \\ a_{16} & a_{15} & a_{14} & \ldots\ldots\ldots\ldots 0 & 0 \\ . & . & . & \ldots\ldots\ldots\ldots & \\ . & . & . & \ldots\ldots\ldots\ldots & \\ a_1 & 1 & 0 & \ldots\ldots\ldots\ldots 0 & \\ 1 & 0 & \ldots\ldots 0 & \ldots\ldots\ldots\ldots 0 & \end{bmatrix} \quad (40)$$

Where a_i's are the coefficients of the characteristic polynomial equation which is:

$$\left|SI - A\right| = S^{20} + a_1 S^{19} + a_2 S^{18} + \ldots + a_{19} S + a_{20} \quad (41)$$

Where I is the unity matrix and by substitution by I and A the coefficients will be calculated from the characteristic equation. And then a new state vector is given by

x = T.$\hat{x}$ (42)

Then, substitution in equation (33), it will be:

$$\dot{\hat{x}} = T^{-1}AT\hat{x} + T^{-1}Bu \quad \text{(the canonical form)} \quad (43)$$

Where

$$T^{-1}AT = \begin{bmatrix} 0 & 0 & 0 & 0\ldots\ldots\ldots\ldots 0 \\ 0 & 1 & 0 & 0\ldots\ldots\ldots\ldots 0 \\ 0 & 0 & 1 & 0\ldots\ldots\ldots\ldots 0 \\ 0 & 0 & 0 & 1\ldots\ldots\ldots\ldots 0 \\ \ldots\ldots\ldots\ldots\ldots\ldots\ldots\ldots\ldots\ldots & & & & \\ \ldots\ldots\ldots\ldots\ldots\ldots\ldots\ldots\ldots\ldots & & & & \\ 0 & 0 & \ldots\ldots\ldots\ldots\ldots\ldots\ldots\ldots & & 1 \\ -a_{20} & -a_{19} & -a_{18} & \ldots\ldots\ldots\ldots\ldots\ldots & -a_1 \end{bmatrix} \quad (44)$$

And also

$$T^{-1}B = \begin{bmatrix} 0 \\ 0 \\ 0 \\ .. \\ .. \\ .. \\ 0 \\ 0 \\ 1 \end{bmatrix} \quad (45)$$

Thus, equation (41) has been transformed to the controllable canonical form taken into consideration that the system is completely state controllable. Then chosen a set of the desired eigenvalues as μ1, μ2,,μ3 …….. and μ20, and by substitution, then the characteristic equation will be in the form

$$(S - \mu_1).(S - \mu_2).(S - \mu_3)\ldots(S - \mu_{20}) = S^{20} + \alpha_1 S^{19} + \alpha_2 S^{18} + \ldots + \alpha_{19} S + \alpha_{20} = 0 \quad (46)$$

Where, α_1 , α_2 ….α_{20} are the coefficients of the desired equation and finally, the desired feedback gain matrix becomes

K = [(α_{20} –a_{20}) (α_{19} –a_{19})…… (α_1-a_1)]. T-1 (47)

Where T^{-1} is the inverse of the transformation matrix.

K = [K1 K2 K3 K4 ……..K20].T^{-1} (48)

Where K1 = α_{20} –a_{20}
K2 = α_{19} –a_{19} .
. K20 = α_1-a_1

.

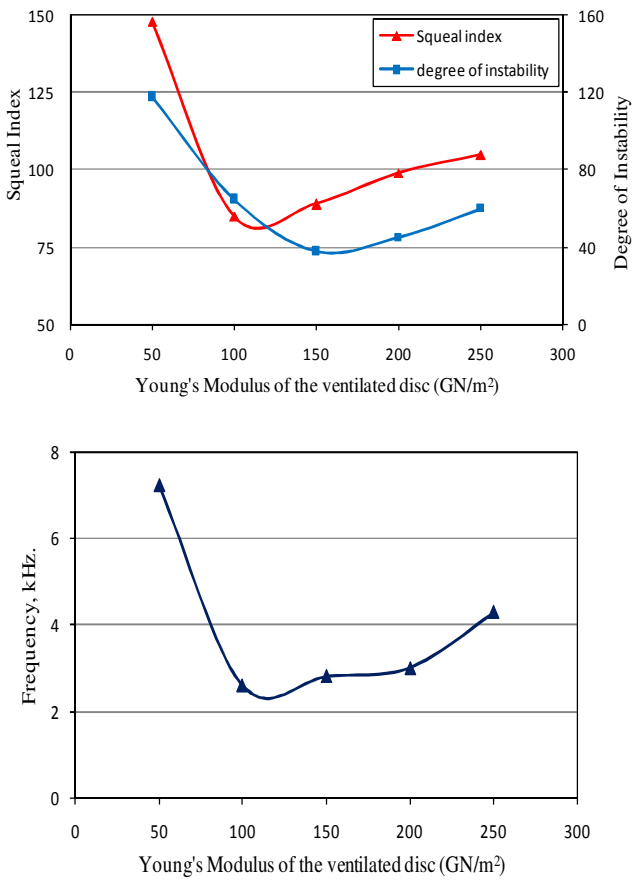

Figure 4. Effect of Young's modulus of brake rotor on brakesqueal noise, degree of instability and frequency respectively.

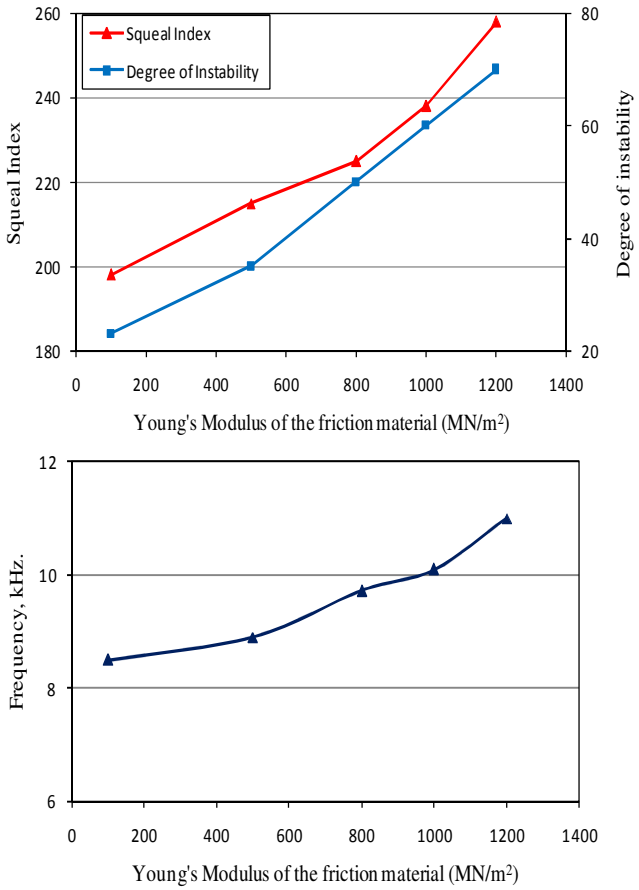

Figure 5. Effect of Young's modulus of friction material on brake squeal noise, degree of instability and frequency respectively.

RESULTS AND DISCUSSIONS

Figure 4 indicates the effect of the Young's modulus of the ventilated rotor on brake squeal noise and degree of instability. The modulus of elasticity of the ventilated brake rotor is increased from 50 to 250 GN/m^2. It can be noted from the figure that as the young's modulus of the rotor increases from 50 to 100 GN/m^2 the squeal index decreases from 148 to 85 and when the young's modulus of the rotor increases from 100 to 250GN/m^2 the squeal index increase from 85 to 105 giving the best value between 90 and 130 GN/m^2. The maximum squeal index of 148 happened with a low modulus of elasticity of 50 GN/m^2 and the lower value of squeal index of 85 and 89 occurred at a rotor Young's modulus of 90 and 130 GN/m^2 respectively. The maximum frequency of 7250 Hz is at rotor young's modulus of 50 GN/m^2 decreases to 2600 Hz at 100 GN/m^2 and then decreases again to be 4300 Hz at rotor young's modulus of 250 GN/m^2.

However the maximum instability of 118 (Real Part) is predicted at rotor young's modulus of 50 GN/m^2 as shown clearly in figure 4. This is to confirm the need for a mean value of the rotor young's modulus to compromise between the performance of the brake and the squeal occurrence.

Figure 5 indicates the effect of the Young's modulus of the friction material on brake squeal noise and degree of instability. The figure shows that as the young's modulus of the friction material increases from 100 MN/m^2 to 1200 MN/m^2 the squeal index increases from 198 to 258 however, the degree of instability increase from 23 to 70. The maximum squeal index 258 occurred at a high modulus of elasticity of 1200 MN/m^2 and the lowest value of squeal index of 198 is predicted at modulus of elasticity of 100 MN/m^2. A frequency of 8500 Hz is predicted at a friction material young's modulus of 100 MN/m^2 and a maximum frequency of 11 kHz reaches at a friction material young's modulus of 1200 MN/m^2 as indicated clearly in figure 4 at a maximum instability of 70 (Real Part). This curves confirmed the need to some extent to a softer friction material to match between the instability of the brake with the frictional behavior of the pad.

When the semi-distance between the clamping bolts of the caliper increases from 30 to 70 mm as in figure 6 the

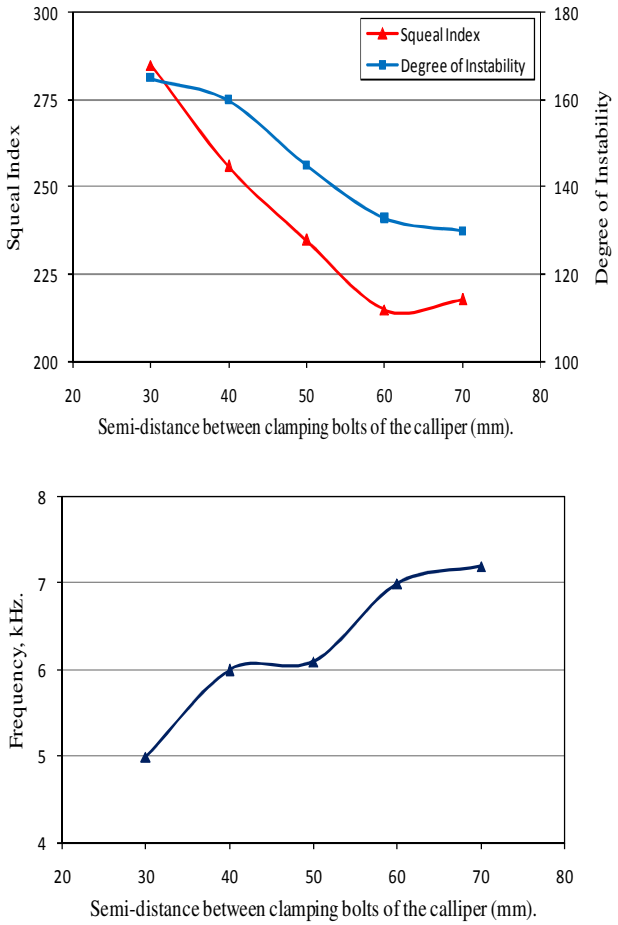

Figure 6. Effect of semi-distance between clamping bolts of the caliper on brake squeal noise, degree of instability and frequency respectively.

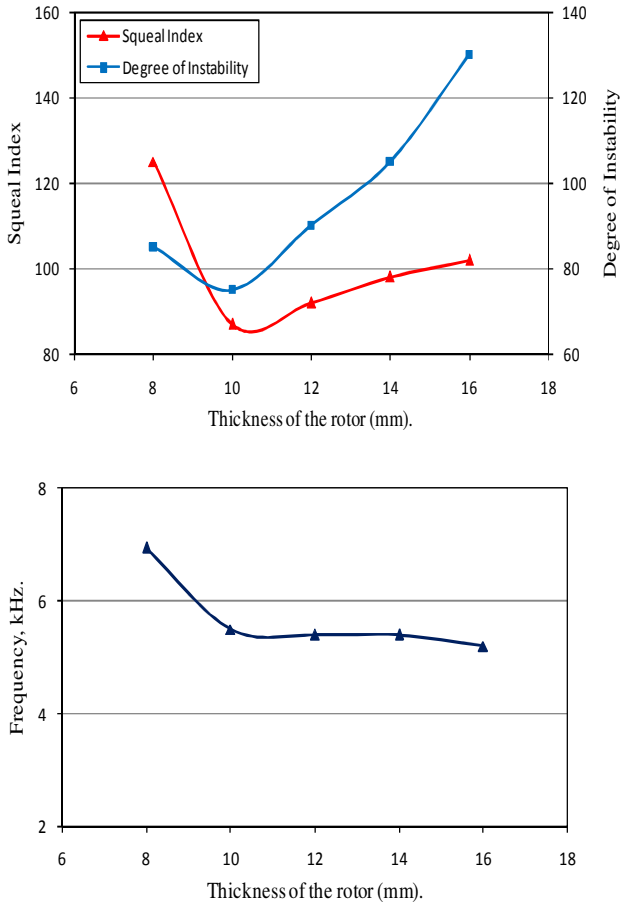

Figure 7. Effect of semi-thickness of brake rotor on brake squeal noise, degree of instability and frequency respectively.

squeal index decreases from 285 to 218 to give the optimum value of the squeal noise at semi-distance between 50 and 70 mm. A minimum value of the squeal index of 215 is predicted at semi-distance of 60 mm and at frequency of 7 kHz as indicated in figure 6. The instability of the system (real part) decreases from 160 to 130 as the semi-distance between the clamping bolts increases. However, the lowest instability of 130-133 (real part) is also calculated at 60-70 mm of the semi-distance between clamping bolts of the caliper. It is normally chosen in most of vehicles in the range of 40-70 mm to overcome the torque generated on the brake due to the brake (piston load) effect. In addition to that the increase of this value could affect the size of the caliper and hence the weight of the caliper which could lead to an added instability.

Figure 7 shows that as the thickness of the upper or lower rings of the ventilated rotor increases between 8-10 mm the squeal index decreases from 125 to 87 and the instability of the system also decreases from 85 to 75. When the thickness of the upper or lower of the ventilated rotor increases from 10 to 15 mm, the squeal index increases from 87 to 102 and the instability will also increase from 75 to 130. Increasing the thickness from 10 to 15 mm affect the natural frequency of the system to decrease from 6590 to 5200 Hz. The increase in the thickness of the upper or lower ring of the rotor above 10 mm lead to a more squeal and instability of the system and this could be due to the effect the rotor thickness on the mode generated from the rotor rotation.

Figure 8 indicates that as the width of the friction material increases from 20 to 30 mm the squeal index increases from 122 to 124 and the instability decreases from 33 to 31 however; the frequency of the system increases from 3500 to 4500 Hz. The squeal index decreases from 124 to 82 when the friction material width increases from 30 to 60 mm and the instability of the system decreases from 31 to 12 indicating the lowest instability of the system. The frequency increases from

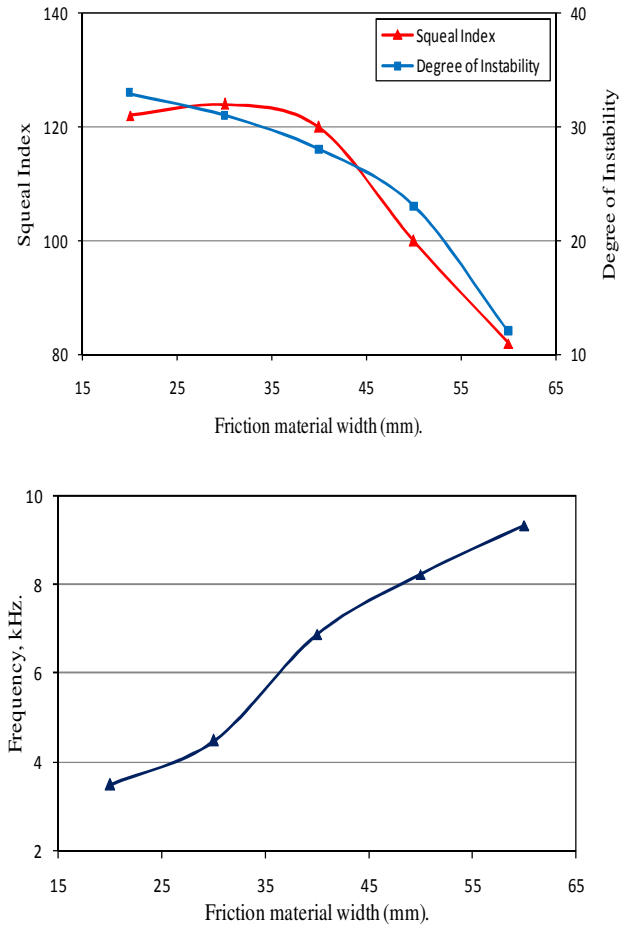

Figure 8. Effect of friction material width on brake squeal noise, degree of instability and frequency respectively.

4500 to 9350 Hz when the width of the friction material increases from 30 to 60 mm. The lower squeal index of 82 is achieved at a friction material width of 60 mm however; the higher of squeal index of 124 is achieved at friction material width of 30 mm at 4500 Hz and instability of 31 (real part) as clear in figure 8.

It is realized from this theoretical analysis that there are some parameters which affect the squeal index and degree of instability of the brake system assembly. Choosing the appropriate specification of the ventilated disc brake components such as mass, young's modulus, stiffness and dimensions of the brake might be useful to control the squeal index and instability of the brake system. For example, increasing the distance between clamping bolts of the caliper will improve the instability of the brake but on the other hand it will affect the caliper weight and stiffness. So, it is recommended to match between the different parameters of the brake system to make a balance between the squeal index and degree of instability and on the other hand the brake performance which is the main challenging issues for brake manufacturers.

The response of the system was obtained by using Simulink in the Matlab program. The figures (9-18) indicate the response of the system with time. It was clear that, by applying a feedback control to the system state (the system assumed to be state controllable), the settling time for all states ranging from 1.5 to 2 seconds is determined depending on the desired poles for the system. Also, the gain matrix K is not one for any system but depends mainly on the desired closed-loop poles locations, which determine the damping of the system and also the speed. By choosing these poles, the system has quite acceptable response characteristics. Because of the system is 20 × 20 matrix, so it was very difficult to determine the poles so, the response characteristics of the system has been checked a lot of times with several different gain matrix K to give the acceptable response.

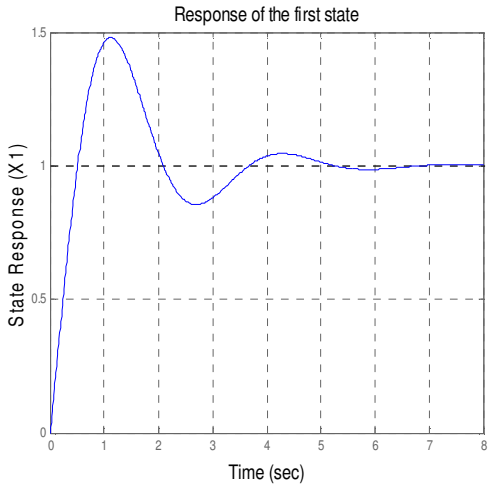

Figure 9. Response of the first state (X1).

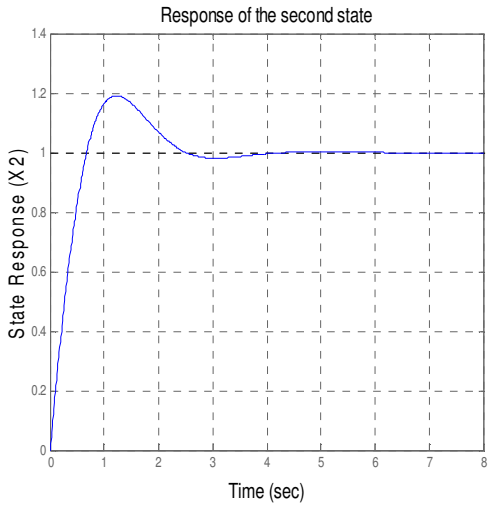

Figure 10. Response of the second state (X2).

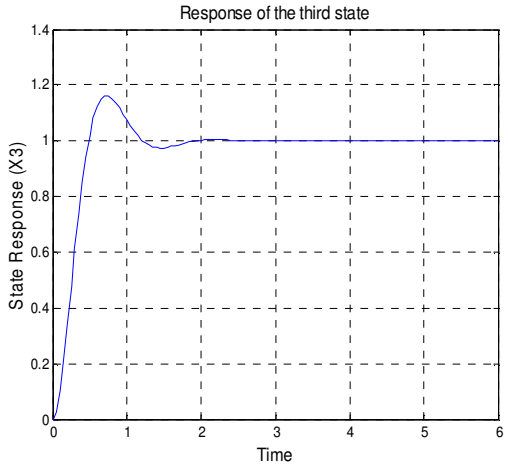

Figure 11. Response of the third state (X3).

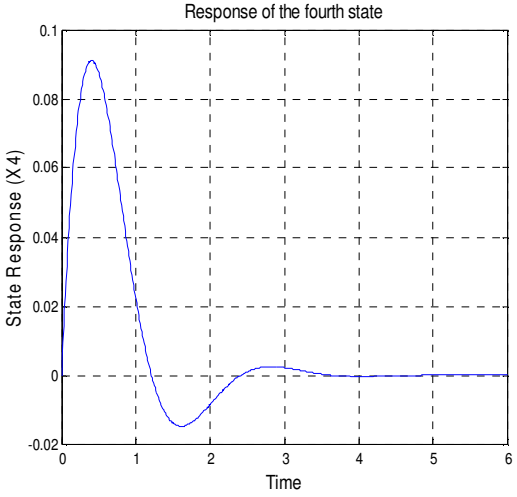

Figure 12. Response of the fourth state (X4).

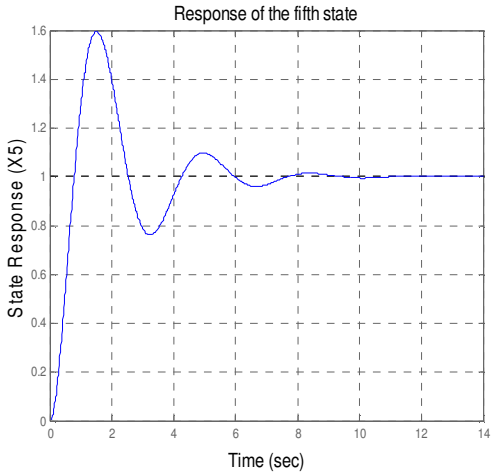

Figure 13. Response of the fifth state (X5).

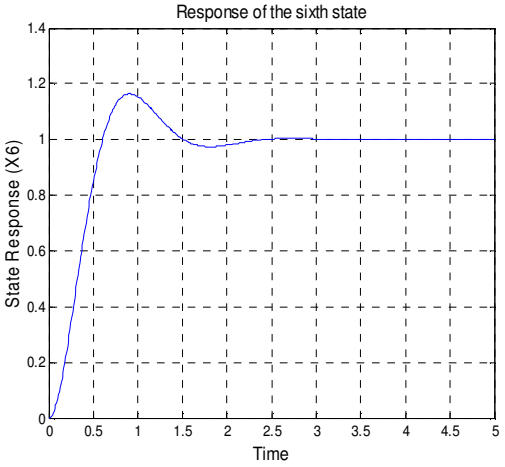

Figure 14. Response of the sixth state (X6).

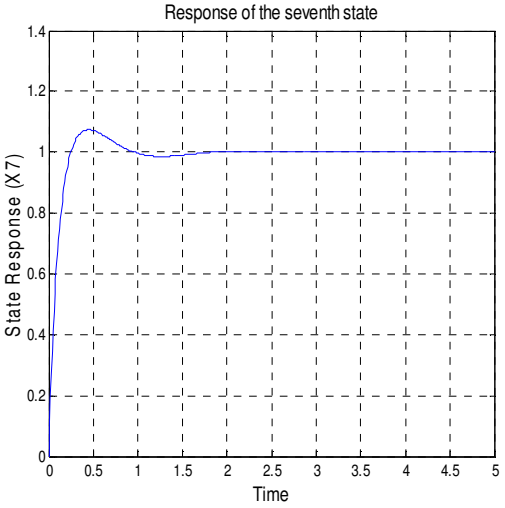

Figure 15. Response of the seventh state (X7).

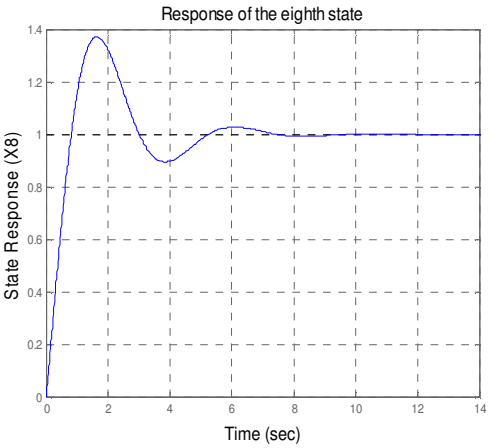

Figure 16. Response of the eighth state (X8).

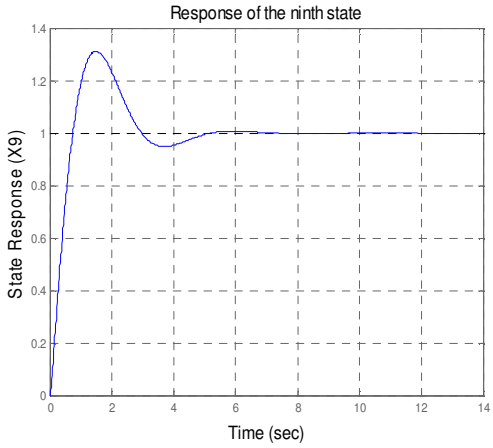

Figure 17. Response of the ninth state (X9).

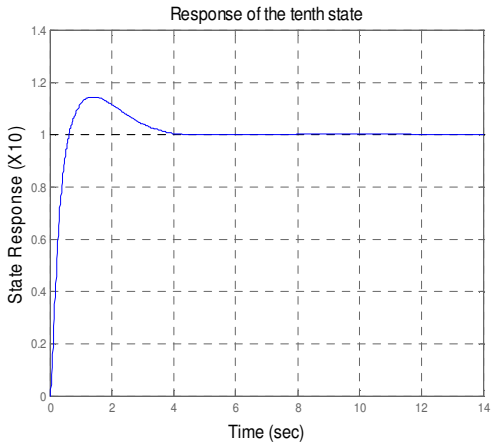

Figure 18. Response of the tenth state (X10).

In terms of squeal tendency after applying the feedback control of the system, that is shown in the following formula:

$$TOI = \sum_i \left(\frac{\text{Realpart } (S_i)}{\text{Imaginarypart } (s_i)} \times 1000 \right), \quad (49)$$

This correlation was used by (Dihua *et al.,* 1998) to show the effect of varying each of these parameters on the tendency of the squeal as a percentage. The physical meaning of the term (Real part (s_i) / Imaginary part (s_i)) is the damping ratio. That a mode had eigenvalue whose real part was above zero meant the system is unstable and the damping value of that mode is negative. Figure 19 shows the squeal tendency against the actual value of the used disc brake, at changing only one parameter such as the Young's Modeulus of the friction material (FR-YM) the squeal tendency is 82%. The tendency of squeal is 75% at using the optimum value of the rotor Young's Modulus (rotor YM). It shows also the squeal tendency at using the optimum values of all the previous components with feedback control is 43% which is the lowest predicted value.

The effect of varying all of the used parameters is presented in this section. Plots of the degree of instability versus frequency of the system at varying these parameters are shown in figure 20. It shows the system instabilities are as less as possible at the ideal predicted,

it is agreeing with all brake noise studies performed in the past as clearly shown in figure 21 which is a typical

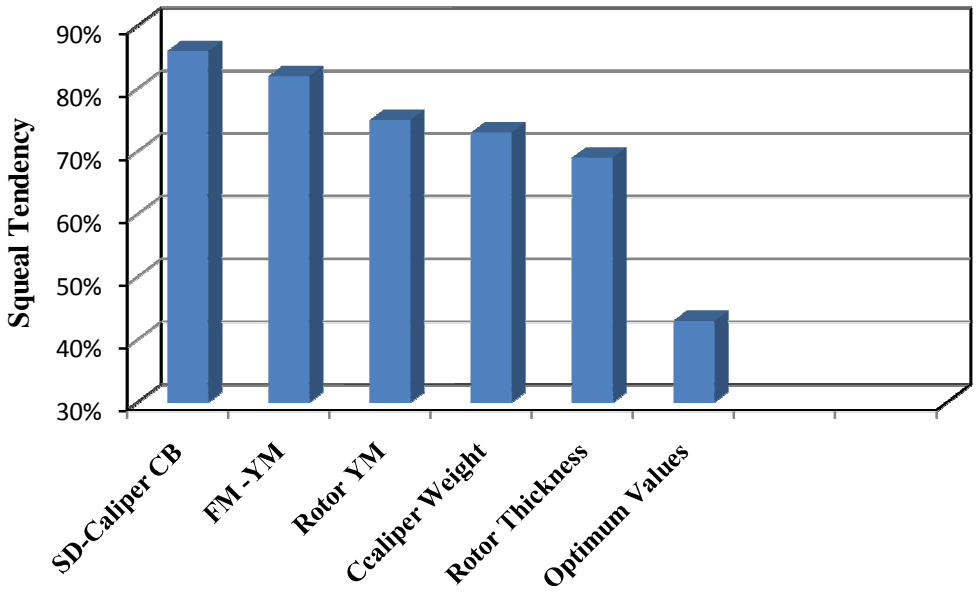

Figure 19. Effect of changing parameters on the squeal tendency.

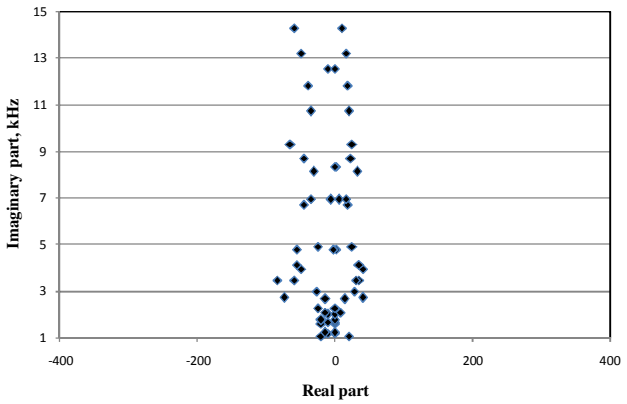

Figure 20. Typical complex eigenvalue plot.

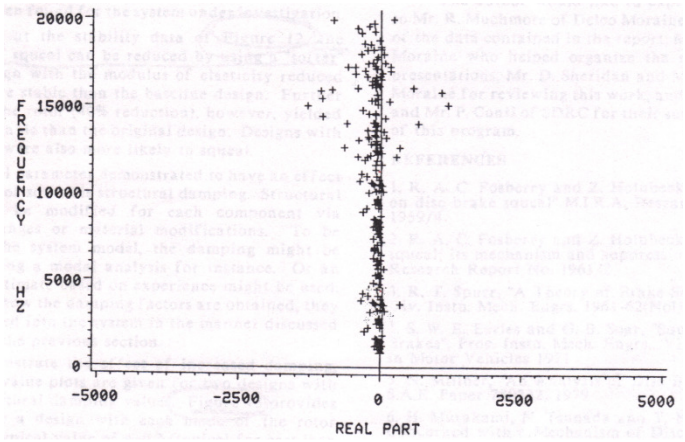

Figure 21. Typical complex eigenvalue plot, (Liles, 1989).

complex eigenvalue plot for (Liles, 1989). Liles varied some parameters in his study seeking to reduce the brake squeal but with a different strategy.

CONCLUSIONS

It is clear from this study that the analytical complex eigenvalue analysis of the ventilated disc brake systems is a very important tool to predict the generation tendency of brake to squeal which is still a very big challenging issue in the car industry and particularly the comfort of the passengers. Different design parameters such as the Young' modulus, thickness of the rotor and friction material, and the width and weight of the friction material were used in this investigation to study their effect on brake squeal in the matter of squeal index and degree of instability. Other parameters were also taken into account in studying the squeal of the brake such as weight and semi-distance between the clamping bolts of the caliper. The following conclusions can be drawn.

- In general, the unstable frequencies calculated by MATLAB program can help in reducing the squeal tendency of the brake system.
- Increasing the Young's modulus (YM) of the ventilated rotor affected the system tendency to squeal behaviour and the optimum value of the rotor YM was between 90 and 130 GN/m^2. The lowest squeal index of 85 and 89 occurred at a rotor YM of 90 and 130 GN/m^2 respectively. However the maximum frequency reached during this change was 7250 Hz.
- Increasing the Young's modulus of the friction material increased the squeal index of the brake system and hence affected the system tendency to squeal. The lowest value of squeal index of 198 was recorded at a YM of 100 GN/m^2. The maximum frequency reached was 11 kHz at a maximum degree of instability of 70 (Real Part). The harder the friction material, the bias of the brake to squeal.
- When the caliper weight increased from 1 to 3 kg the squeal index (SI) decreased from 155 to 85 and when it increased from 3 to 5 kg the SI increased from 85 to 112. Increasing the semi-distance between the clamping bolts of the caliper decreased the SI noise of the brake system assembly and also decreased the degree of instability of the brake system.
- Increasing or decreasing the semi-distance between clamping bolts of the calliper had a great effect on the tendency of squeal. Increasing the semi-distance from 30 to 70 mm decreased the squeal index from 285 to 218. The optimum semi-distance between clamping bolts of the calliper was 70 mm. It is recommended to be in the range of 40-70 mm because over increase of this value will affect the squeal occurrence.
- The thickness of the upper or lower rings of the ventilated rotor had a major effect on the brake squeal index. The minimum squeal index of 87 happened with a rotor thickness 10 mm and frequency of 5500 Hz. When the thickness increased above 10 mm the squeal index increased rapidly.
- Controlling the output signal of the system by using the pole placement give a better response to the system depending on the desired poles which determines the damping and the speed of the response.
- The predicted squeal tendency at varying all the studies parameters with feedback control signal is as less as possible to be 43 % compared to other single parameters without control signal.

REFERENCES

Ahmed A.A. Saad, Ibrahim Ahmed and Mohamed Watany "Automotive Disc Brake Occurrence: An Experimental Investigation" Engineering Research Journal 119 (October 2008) M1-M20, Helwan University, Cairo, Egypt, 2008.

Crolla, D. A. "Automotive Engineering powertrain, chassis system and vehicle body" ISBN: 789-85617-577-7, Elsevier Inc., 2009.

Dai Y. and Lim T.C. "Suppression of brake squeal noise applying finite element brake and pad model enhanced by spectral-based assurance criteria" Applied Acoustics, Vol. 69, pp. 196–214, 2008.

Dihua D. and Dongying J. "A Study on Disc Brake Using Finite Element Methods" SAE, No. 980597, pp 157-163, 1998.

Earles S.W., and Chambers P.W. "Disc Brake Squeal- some factors which influence its occurrence" IMechE, C454/88, pp 39-46, 1988.

Hu, Y., Mahajan, S., and Zhang, K. "Brake squeal DOE using nonlinear transient analysis" SAE Paper 1999-01-1737, 1999.

Ibrahim Ahmed "Analysis of disc brake squeal using a ten-degree-of-freedom model" International Journal of Engineering, Science and Technology, Vol. 3, No. 8, pp. 142-155, 2012.

Ibrahim Ahmed, Sameh Metwally, Eid Mohamed and Shawki Aouel-Seoud "Influence of Surface Modification on Vehicle Disc Brake Squeal" SAE 2009-01-1977, SAE 2009 International Powertrains Fuels and Lubricants Meeting, June 15-17, 2009.

Kinkaid N. M., O'Reilly O.M. and Papadopoulos P., "Review of Automotive Disc Brake Squeal" Journal of Sound and Vibration, 267, 105-166, 2003.

Lee, Y.S., Brooks, P.C., Barton, D.C., and Crolla, D.A. "A Study of Disc Brake Squeal Propensity Using a Parametric Finite Element model" European Conference on Vehicle Noise and Vibration, IMechE, C521/009/98, 1998.

Liles GD. Analysis of disc brake squeal using finite element methods. Technical Report SAE 891150, 1989.

Liu, P., Zheng, H., Cai, C., Wang, Y.Y., Lu, C., Ang, K.H., Liu, G.R. 2007. Analysis of disc brake squeal using the complex eigenvalue method, Applied Acoustics, Vol. 68, pp. 603–615.

Mario Triches Junior, Samir N.Y. Gerges and Roberto Jordan "Analysis of brake squeal noise using the finite element method: A parametric study" Journal of Applied Acoustics 69 (2008) 147–162, 2008.

Masaaki Nishiwaki, Hiroshi Harada, Hiromasa Okamura, and Takahiro Ikeuchi "Study on Disc Brake Squeal" SAE, No. 890864, pp 980-989, 1989.

Millner, N. "An Analysis of Disc Brake Squeal." SAE, No. 780332, 1978.

Moriaki Gouya, and Massaki Nishiwaki "Study on Disc Brake Groan" SAE, No. 900007, pp 16-22, 1990.

Neubauer, M., Kröger, M.: Brake squeal control with shunted piezoceramics - Efficient modeling and experiments - In: Journal of Automobile Engineering, Proceedings of the Institution of Mechanical Engineers Part D, Vol. 222, Number D7, ISSN 0954-4070, pp. 1141-1152, 2008.

North M.R. "Disc Brake Squeal- A Theoretical Model" MIRA Report, No. 1972/5.

Ogata K., "System dynamics" third edition, Prentice-Hall International Limited, London, UK, 1998.

Saw Chun Lin, Abd Rahim Abu Bakr, Wan Mohd Mysyris, Badri Abd Ghani and Mohd Rahimi Jamaluddin "Suppressing Disc Brake Squeal Through Structural Modifications" Journal Mekanikal, December 2009, No. 29, 67-83, UTM, Malysia, 2009.

Shin, K., Brennan, M.J., Oh, J.-E., Harris, C.J."Analysis of disk brake noise using a two-degree-of-freedom model" Journal of Sound and Vibration, Vol. 254, No. 5, pp. 837–848, 2002.

Thomas G. Carne, and Clark R. Dohrmann "Support Conditions, Their Effect on Measured Modal Parameters" Proceedings of the 16th International Modal Analysis Conference- Santa Barbara-California IMAC-1998 volume I, 1998.

Utz von Wagner, Daniel Hochlenert, Thira Jearsiripongkul and Peter Hagedorn "Active control of brake squeal via "smart pads" SAE 2004-01-2773, 2004.

William J. Bracken and Johnny K. Sakioka "A Method for the Quantification of Front Brake Squeal" SAE, No. 820037, pp 142-149, 1982.

Yasuaki Ichiba, and Yuji Nagasawa "Experimental Study on Disc Brake Squeal" SAE, No. 930802, pp 1227-1234, 1993.

Yukio Nishizawa, Hironobu Saka, Shiro Nakajima, and Takeo Arakawa "Electronic Control Cancelling System for a Disc Brake Noise" SAE, No. 971037, pp 83-88, 1997.

NOMENCLATURE

a	Rotor fins height
b	Semi-length of the caliper piston.
C_1	Linear damping between the rotor and the right pad.
C_2	Linear damping between the rotor and the left pad.
C_3	Linear damping between the right pad and right caliper
C_4	Linear damping between the left pad and the left caliper
C_D	Linear damping of the rotor.
Cc	Linear damping of caliper.
C_5	Rotary damping of the right pad.
C_6	Rotary damping of the left pad.
C_7	Rotary damping of the right caliper piston.
C_8	Rotary damping of the left caliper piston.
C_{RD}	Rotary damping of the rotor.
C_{RC}	Rotary damping of the caliper.
d	Semi-thickness of the pad.
Ed	Young's modulus of the disc (rotor).
Ep	Young's modulus of the pad.
$F1,F2$	Contact forces.
h	Thickness of the upper and lower ring of the ventilated
I_d, I_P,I_C	Moment of inertia of the rotor, pad and caliper
K_1	Linear stiffness of right pad.
K_2	Linear stiffness of the left pad.
K_3	Linear stiffness between the right pad and the piston.
K_4	Linear stiffness between the left pad and the piston.
K_D	Linear stiffness of the rotor.
Kc	Linear stiffness of the caliper piston.
K_5	Rotary stiffness of the right pad.
K_6	Rotary stiffness of the left pad.
K_7	Rotary stiffness of the right caliper piston.
K_8	Rotary stiffness of the left caliper piston.
K_{RD}	Rotary stiffness of the rotor.
K_{RC}	Rotary stiffness of the caliper.
M_d, M_P, M_C	Mass of the disc (rotor), pad and caliper respectively.
r_i, r_o	Inner and outer radius of the ventilated rotor respectively.
x_d	Displacements of the ventilated rotor.
x_1	Displacements of the right pad.
x_2	Displacements of the left pad.
x_3	Displacements of the right caliper piston.
x_4	Displacements of the left caliper piston.
μ	Coefficient of friction of the friction material.
ρ,ρ_p	Density of the disc (rotor) and the pad respectively.
θ_1	Angle of rotation of the right pad around y-axis.
θ_2	Angle of rotation of the left pad around y-axis.
θ_3	Angle of rotation of the right caliper piston around y-axis.
θ_4	Angle of rotation of the left caliper piston around y-axis.
θ_d	Angle of rotation of the rotor around y-axis.